



Thermally stable and durable superhydrophobic surfaces on stainless steel sheets with microholes via acid pretreatment and modification with self-assembled monolayers

Muhammad Omar Shaikh¹ · Jia-Yu Yang² · Cheng-Hsin Chuang²

Received: 5 June 2021 / Accepted: 6 October 2021 / Published online: 16 October 2021
© The Author(s), under exclusive licence to Springer-Verlag GmbH Germany, part of Springer Nature 2021

Abstract

In this study, we investigate the use of a facile two-step protocol to develop thermally stable and durable superhydrophobic (SH) surfaces on stainless steel (SS) that can strongly repel aqueous media. This involves pretreatment to achieve enhanced surface roughness using hydrofluoric acid etching followed by covalent modification with long-chain fluorosilanes which form a self-assembled monolayer (SAM) and reduce the surface energy of the SS. Experimental results show that hydrofluoric acid etching can increase the surface roughness and density of hydroxyl groups, thus enabling successful SAM adsorption. The SAM coating time, temperature and concentration have also been optimized to achieve dense and uniform coverage on the surface. It was observed that increasing the SAM concentration and temperature can effectively increase the interaction rate of SAM molecules with the S.S surface, thus resulting in a denser coverage and faster film formation rate. The proposed protocol in this study can successfully increase the hydrophobicity of the SS surface with an observed water contact angle as high as 170° and no significant loss in performance after several months of manufacture and exposure to temperatures up to 300 °C. Furthermore, we have laser machined an array of microholes in SS sheets and have investigated the feasibility of our protocol to achieve IPX7 waterproof rating when the sheets are submerged at a depth of 1 m underwater for 30 min. It was observed that water did not penetrate through the microholes with a diameter of 10 μm or less even at hydrostatic pressures of 1 m, thus highlighting the practical applicability of the proposed protocol to fabricate SH surfaces on SS for use in healthcare and industry.

Keywords Superhydrophobic · Stainless steel · Pretreatment · HF acid etching · Self-assembled monolayers

1 Introduction

Stainless steel (SS) in its various forms has several applications in our modern world ranging from industry to healthcare (Cobb 2010; Khatak et al. 2002). While SS has excellent mechanical properties and resistance to high temperatures, it can become contaminated with microorganisms like bacteria and fungi or can undergo corrosion over time in the presence of corrosive media (Duarte et al. 2013; Abdallah et al. 2014; Ferroni et al. 1998). A proposed solution

to address this issue is the fabrication of superhydrophobic (SH) surfaces on SS which strongly repel water and thus eliminate bioactivity and corrosion. SH surfaces with a static contact angle greater than 150° have attracted significant attention owing to their suitability for enabling diverse applications that require self-cleaning, drag reduction, oil/water separation, anti-bacterial and anti-fouling effects, anti-reflection and corrosion resistance (Kavalenka et al. 2017; Wang et al. 2015, 2017a; Zhang et al. 2016, 2017; Yang et al. 2017a, b; Sun et al. 2014; Shen et al. 2012). SH surfaces are also widely observed in nature with some examples being the water-strider legs, lotus and rice leaves, butterfly wings and rose petals (Zhang et al. 2009; Gao and Jiang 2004; Watson et al. 2015; Feng et al. 2008; Bixler and Bhushan 2012; Bhushan et al. 2009). The low wettability observed in these biological species originates from the enhanced surface roughness due to the presence of nano/microstructures and novel surface chemistries (Zhang et al. 2014; Guo et al.

✉ Cheng-Hsin Chuang
chchuang@imst.nsysu.edu.tw

¹ Sustainability Science and Engineering Program, Tunghai University, Taichung 407224, Taiwan

² Institute of Medical Science and Technology, National Sun Yat-Sen University, Kaohsiung 80424, Taiwan

2011; Liu et al. 2012; Ye et al. 2017). Over the past few decades, there have been research efforts aimed at developing scalable, inexpensive, and high-throughput methods to fabricate SH surfaces on a range of substrates including metals, glass, polymer and fabrics (Ahuja et al. 2008; Bormashenko et al. 2006; Ma et al. 2005; Nakajima et al. 2000; Qian and Shen 2005). Metals such as titanium, copper and aluminum have also been modified to obtain SH properties primarily by introducing surface roughness and modification with organic molecules to reduce surface energy (Qian and Shen 2005; Liu and Jiang 2011).

SS is broadly referred to iron-based metals which contain a chromium content greater than 12%. The composition of SS varies depending on the desired application with different alloys resulting in varying mechanical strength and corrosion. Owing to the extensive applications of SS that require antifouling and corrosion resistance, fabrication of thermally stable and durable SH surfaces on SS is urgently needed. This is particularly applicable for industries and healthcare facilities where metal-fluid contact commonly occurs. Several techniques have been utilized to introduce produce SH surfaces which include plasma/chemical etching, sol-gel methods, templating, electrodeposition, micro milling, nanoimprint lithography and femto, pico and nanosecond pulse laser machining (Hsieh et al. 2008; Wu et al. 2013; Peng et al. 2013; Pozzato et al. 2006; Pan et al. 2013; Nine et al. 2015; Barthwal et al. 2013; Wang et al. 2014, 2017b; Choi et al. 2015; Caldarelli et al. 2015; Li et al. 2014; Long et al. 2016; Martínez-Calderon et al. 2016; Zheng et al. 2016; Zhao et al. 2019; Dunn et al. 2016; Yang et al. 2017c; Kwon et al. 2014). However, many of these techniques face major challenges in the form of either high cost, complex processes, low production efficiency or inadequate stability which are all critical for industrial production of SH surfaces. For instance, femto and picosecond laser machining can produce nano/microstructures with high durability but require expensive instrumentation which hinders scalability. Nanosecond lasers are a relatively lower cost alternative and have been used to pattern roughness structures on SS surfaces with achievable water contact angles higher than 150° (Dunn et al. 2016; Yang et al. 2017c). While nanosecond laser machining is promising, further research is still required to enable optimization and cost reduction as the lasers and their imaging optics are expensive. On the other hand, surfaces that are modified simply using chemical methods or added material to introduce roughness can achieve superhydrophobicity but are prone to low stability and durability. In addition, the adhesion strength between the coating and substrate must be improved to ensure reliable performance.

In this study, we propose a facile two-step protocol to create SH surfaces on 304 SS which consists of a pretreatment using hydrofluoric (HF) acid etching followed by

modification with highly stable fluorosilane based self-assembled monolayers (SAMs) to achieve a low energy surface. 304 SS contains 18% chromium and 8% nickel with the rest being primarily iron. The main goal of the HF acid etching pretreatment is to introduce surface roughness and improve hydroxylation of the SS surface. The HF acid selectively attacks grain boundaries via intergranular corrosion, thus resulting in micro/nano surface roughness. The benefit of introducing surface roughness by directly etching the surface as opposed to material deposition is the inherent mechanical stability that the surface possesses after etching. We have also compared HF acid etching with a UV Ozone (UVO) pretreatment which simply hydroxylates the surface, thus increasing hydrophilicity without affecting the surface roughness. After pretreatment, we modify the SS surface with fluorosilane based SAMs which provide a convenient, simple and low-cost system to tailor the surface properties of metals, metal oxides, and semiconductors. SAMs are organic assemblies formed by the adsorption of molecular constituents from the solution or gas phase onto the surface of solids and a covalent or semi-covalent interaction can be utilized. Previously, a range of surface modification techniques including initial pretreatment steps followed by SAM modification have been utilized to improve the hydrophobicity of SS surfaces (Kim et al. 2018; Li et al. 2012; Zhu et al. 2014). Furthermore, we have also optimized experimental parameters including HF acid etching pretreatment and SAM coating time, temperature, and concentration which all influence the final achievable hydrophobicity of the SS surface. The proposed protocol is simple and effective and can enable large-scale fabrication of thermally stable and durable SH surfaces on SS.

2 Experimental methods

2.1 Materials

304 SS sheets with dimensions of 19 mm \times 19 mm \times 0.5 mm were purchased from Tronway Enterprise Co., Ltd. 1H, 1H, 2H, 2H-Perfluorodecyltriethoxysilane and Hydrofluoric acid were purchased from Sigma-Aldrich. Ethanol and Acetone were purchased from Echo Chemical Co., Ltd. All chemicals were used as purchased without further purification.

2.2 Instruments and characterization

The surface morphology of the SS sheets after HF acid etching was characterized using a scanning electron microscope (SEM, S-3000 N, Hitachi, Japan) and an optical microscope (OM, BX53M, Olympus, Japan). The measurement of surface roughness was performed using an atomic force microscope (AFM, Innova, Bruker, USA).

A comparative pretreatment protocol was performed using a UV-Ozone cleaner (UV-0100, All Real Technology Co., Ltd, Taiwan) which cleans the SS304 organic contaminants and increases the hydrophilicity without affecting surface roughness. The formation of OH groups after the pretreatment steps was measured using an Attenuated Total Reflection Fourier-transform infrared spectroscopy (ATR-FTIR, Frontier, Perkin Elmer, USA) in a scanning range of 650 to 4000 cm^{-1} . The static water contact angle was measured at ambient temperature using a contact angle meter (Theta Lite, Biolin Scientific, Sweden) and the water droplet size was 4 μL . Finally, a 10×10 array of microholes with different diameters (10, 25 and 30 μm) was drilled in the SS304 sheets using a laser drilling protocol made by Crystal Entec Corporation, Taiwan. A1000 grit sandpaper was used to remove the oxide layer that forms on the SS after laser drilling and enable effective pretreatment.

2.3 Pretreatment

The SS sheets were first ultrasonicated in 95% ethanol solution to clean organic contaminants for 10 min then followed by drying using nitrogen gas. This is followed by a pretreatment step using either HF acid etching or UV Ozone to increase the surface OH groups and resulting hydrophilicity so that the SAM can easily be adsorbed on the SS surface. The HF acid etching pretreatment was performed by immersing the SS in 48% HF solution followed by vigorous rinsing with DI water and drying using nitrogen gas. UV-Ozone pretreatment was done by placing the SS in UV ozone for 30 min. A schematic of the complete process including pretreatment protocols used and SAM modification to create SH surfaces on SS is shown in Fig. 1.

2.4 SAM modification

A 50 mM to 200 mM solution of 1H, 1H, 2H, 2H-Perfluorodecyltriethoxysilane solution was first prepared in 95% alcohol under constant magnetic stirring. After 15 min, the pretreated SS sample was placed in the SAM solution for up to 4 h followed by sequential rinsing with alcohol, acetone and deionized water and finally drying with nitrogen gas.

2.5 IPX7 waterproof testing

The International Protection (IP) code is a certification that proves that a product meets certain water/dust proofing criteria. IPX7 which is provided for digital products like smartphones is completely protected from dust and is waterproof tested for a minimum of 30 min underwater at 1 m. We have tested the reliability of our protocol for possible applications which may require IPX7 water-proofing capability but allow air/gas permeation. To simulate IPX7 test conditions, we first use our two-step protocol to modify SS sheets that have an array of microholes obtained using laser drilling. We have made an acrylic vessel using laser cutting to which the SS sheets can be attached as a cover layer as shown in Fig. 2. The silica gel beads increased the weight of the vessel while a filter paper served a calorimetric sensor. The vessel was then inserted and kept for an hour in a vertical column that was filled with red-colored water to a height of 1 m. If the water penetrated through the microholes in the SS sheets, the filter paper would change color to red. Our goal was to test the feasibility of the SH coating to prevent water penetration at pressures of 1 m and optimize the microhole diameter that would enable IPX7 waterproofing capability while allowing for air/gas penetration. To the best of our knowledge, this is the first study of its kind to test industry-standard IPX7 waterproofing for SS surfaces with microholes that possess SH properties.

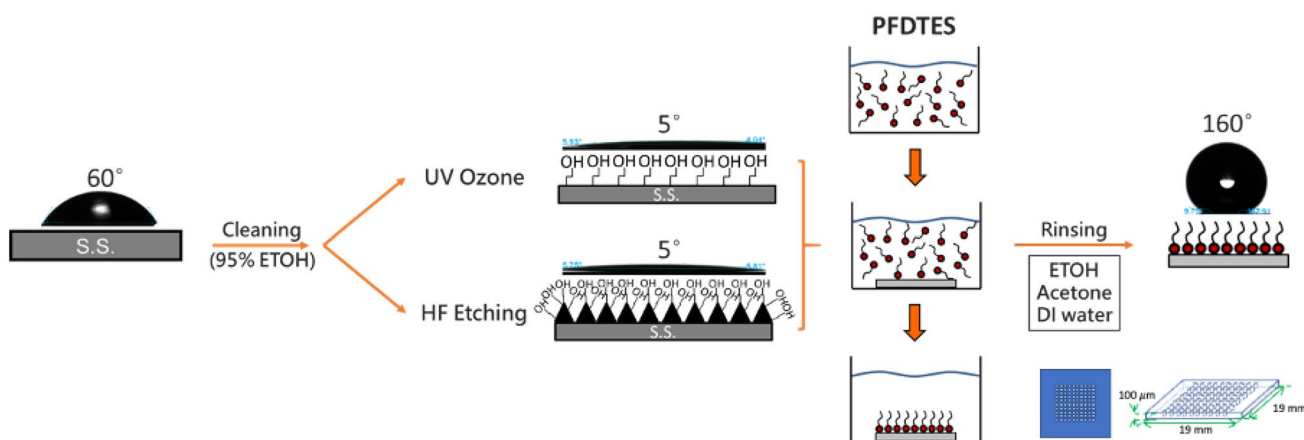


Fig. 1 Schematic of the two-step protocol used to fabricate SH surfaces on 304 SS with an image of the water droplet contact angle at each stage

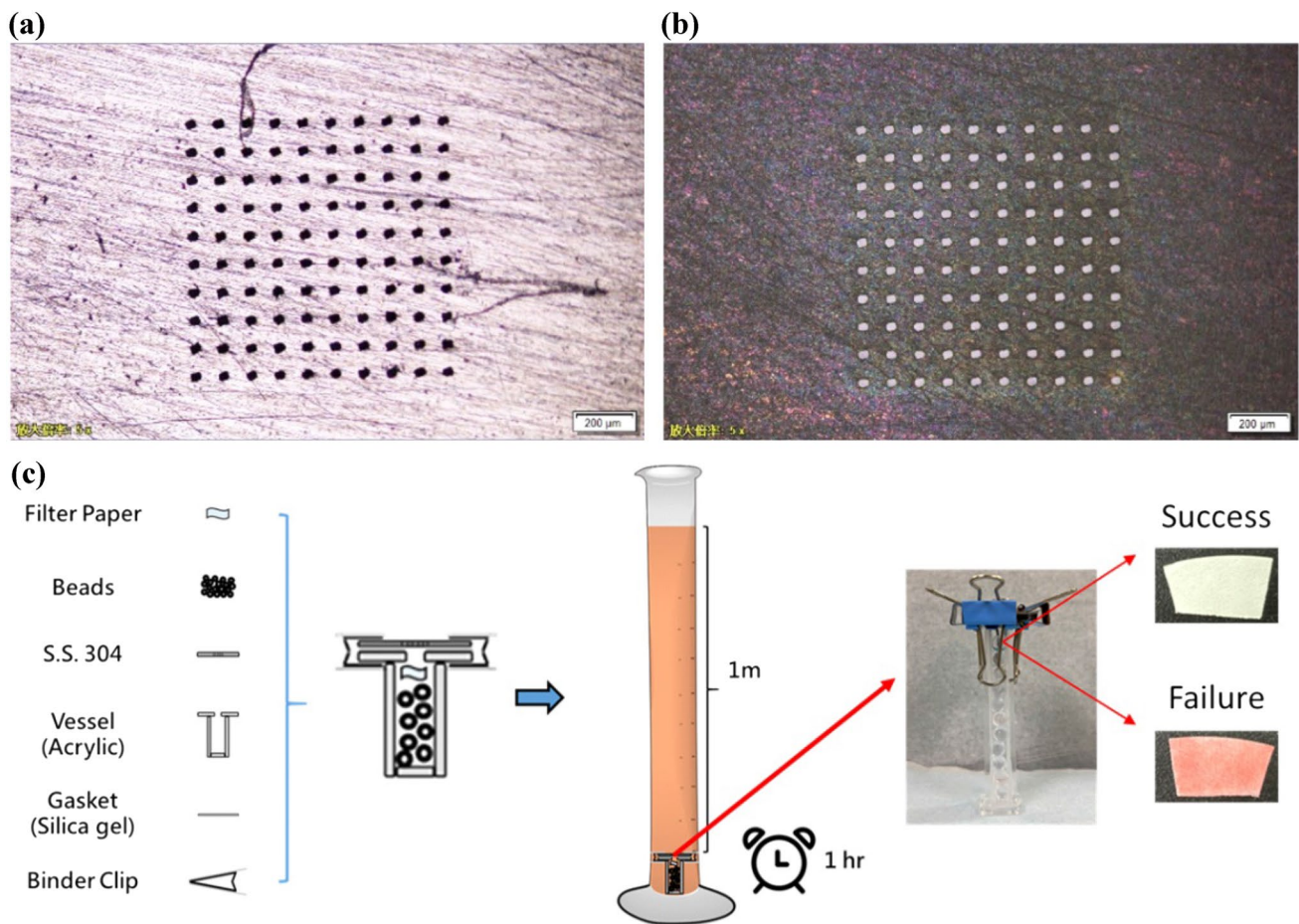


Fig. 2 **a** SS sheet with a 10×10 array of microholes obtained using laser drilling and **b** after HF acid etching pretreatment and SAM modification. **c** Setup used to test the SS sheets with microholes for IPX7 waterproofing feasibility

3 Results and discussion

3.1 Effect of pretreatment protocol

HF acid has commonly been used in the pickling of SS in the presence of nitric acid (HNO_3) to eliminate surface contamination. This process utilizes competing reactions between HF acid etching and HNO_3 passivation which continues until the surface is cleaned. However, when HF acid etching is used without an oxidizer like HNO_3 as done in this study, the corrosive chemical reaction continues without hinderance which results in the formation of a roughened surface. The surface roughness after HF acid etching for a duration of up to 25 min is shown in Fig. 3a while the resulting surface morphology is shown in the SEM and OM images in Fig. 3b. We have utilized an optimized treatment time of 25 min in 48% HF solution to obtain the desired surface roughness without significantly etching the surface and changing the thickness of the SS sheets. After HF acid etching, the SS surface turns black as shown in Fig. 2 due to a change in

surface morphology and chemical composition while the solution turns green due to the presence of iron and chromium fluorides (Li et al. 2012). The HF concentration and etch duration define the size, distribution and stability of the etched structures that result in the surface roughness. Furthermore, it is important to highlight that rigorous rinsing with DI should be performed after the HF acid etching pretreatment to ensure complete hydroxylation of the SS surface which improves hydrophilicity and is critical for improved absorption of the fluorosilane SAM.

We have also compared the HF acid etching pretreatment with UVO which is a simple and rapid method to obtain clean surfaces on substrates like metals, silicon and glass. The UVO treatment removes contaminants from the surface and promotes rehydration which increases the hydrophilicity of the SS. It should be noted that the UVO treatment is gentle and does not etch the surface of the SS. The surface morphology of the SS after UVO treatments for 15, 30 and 60 min are shown in the SEM images in Fig. 3c. Compared to the blank SS, no significant change

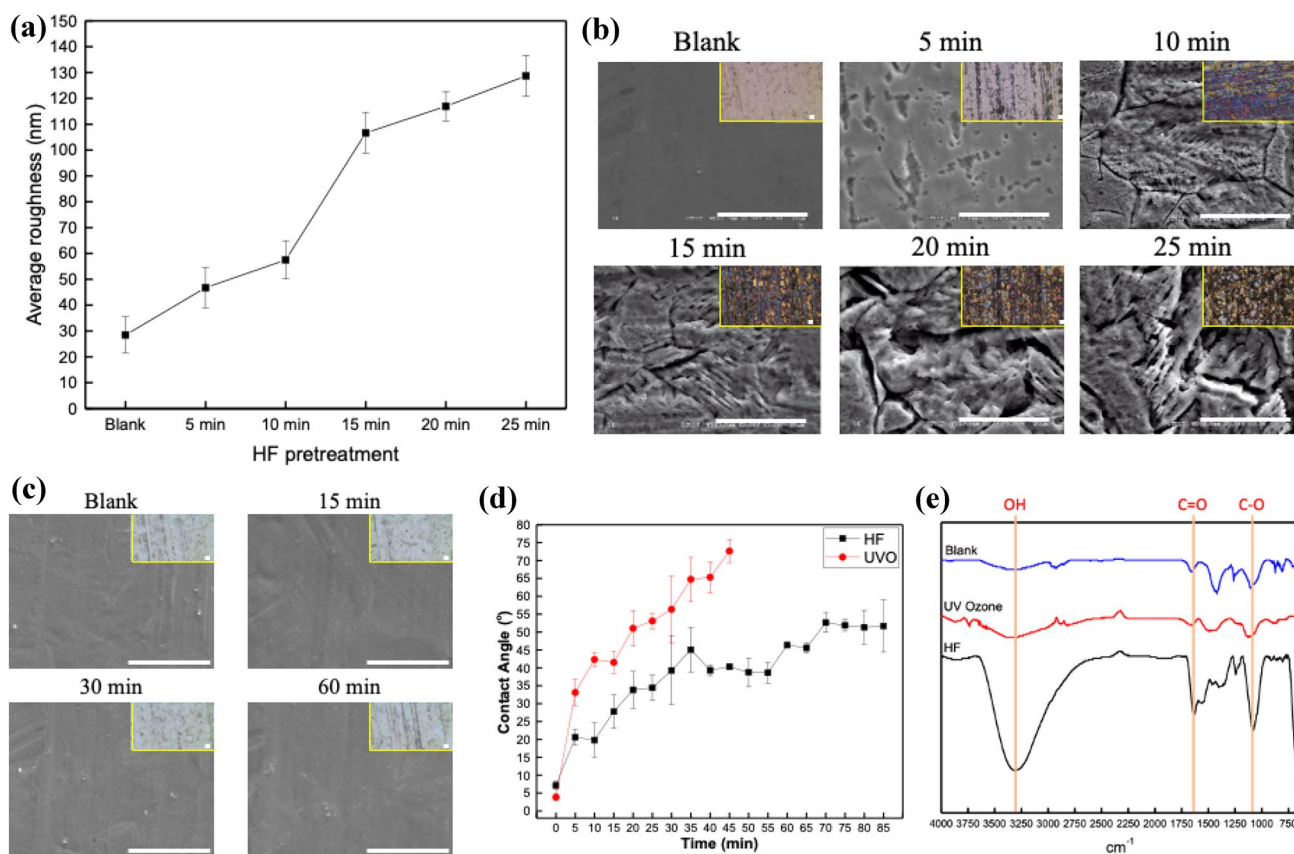


Fig. 3 Effect of **a** HF acid etching time on the surface roughness of SS. **b** The resulting SEM and OM (inset) images of the HF etched SS surface where the scale bar corresponds to 10 μm. **c** The resulting SEM and OM (inset) images of the UVO treated SS surface where

the scale bar corresponds to 10 μm. **d** The observed contact angle of HF acid etching and UVO pretreatments after exposure to air for different time durations. **e** The resulting FTIR spectra for blank and pretreated SS sheets

in surface morphology was obtained after the UVO treatment. The resulting water contact angles obtained for the two pretreatments after exposure to air for different time durations are shown in Fig. 3d. It was observed that the water contact angle drops dramatically to below 10° after 1 min and increases thereafter with exposure time. This implies that the SAM immobilization should be performed immediately after pretreatment when the surface is superhydrophilic. Furthermore, ATR-FTIR results as shown in Fig. 3e confirm the presence of OH functional groups after both HF acid etching and UVO treatment. However, the increase in OH peak is significantly higher after the HF acid etching as compared to the UVO treatment. This suggests that the SS surface becomes more hydrophilic after HF acid etching and consequently should adsorb more SAM on the surface. This could be associated with the increased surface roughness produced during etching which does not occur during UVO.

3.2 Effect of SAM immobilization time, temperature and concentration

We have also optimized the experimental parameters during SAM immobilization which include immobilization time, temperature and SAM concentration as shown in Fig. 4. These tests were conducted using 304 SS sheets without any pretreatment. We tested SAM immobilization time up to 24 h and found that about 4 h is sufficient to achieve a dense coverage and a final contact angle of about 110°. Next, we tested different SAM solution temperatures ranging from 25 to 75 °C. Increasing the temperature increases the kinetic energy of the SAM molecules and enables them to interact with SS surface more frequently. It was observed that a solution temperature of 50 °C was enough to achieve complete SAM saturation on the SS surface and result in a contact angle of about 120°. Finally, we have also utilized different SAM concentrations ranging from 10 to 200 mM.

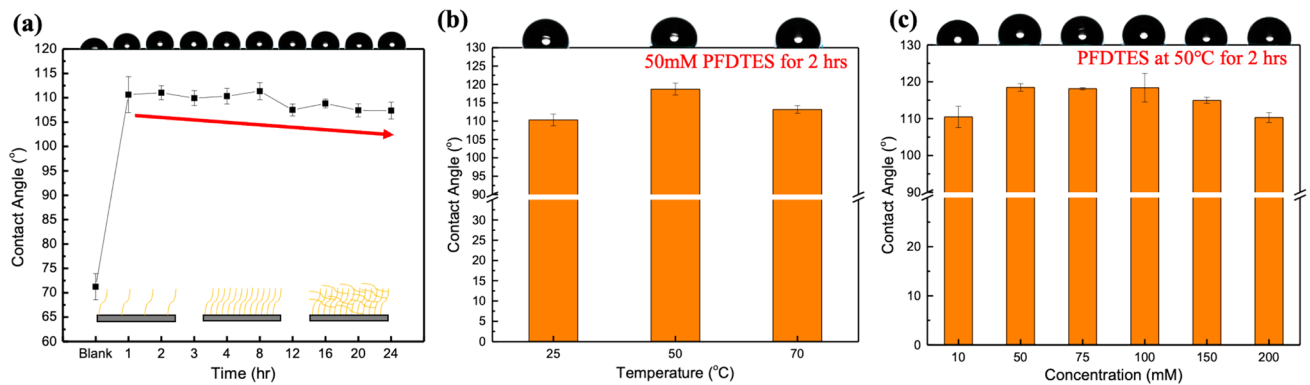


Fig. 4 Optimization of SAM immobilization protocol using different **a** Immobilization time **b** Temperature and **c** SAM concentration

We observed that a concentration of 50 mM was enough to achieve SAM saturation and result in a final contact angle of about 120°. We have used these optimized parameters for SAM immobilization in the two-step protocol to achieve SH surfaces on stainless steel.

3.3 Feasibility of the proposed two-step protocol

Finally, we have tested the feasibility of the proposed two-step protocol to obtain SH surfaces on stainless steel. This involves the HF acid etching and UVO pretreatments followed by SAM immobilization and the final observed water contact angle was measured as shown in Fig. 5a. SS samples with UVO treatment of 30 min and HF acid etching for 5 min and 25 min were compared, and the resulting contact angles observed after SAM immobilization were 119°, 146° and 170°, respectively. These results confirmed that HF acid etching pretreatment was more suitable for achieving superhydrophobicity after SAM immobilization. Furthermore, to ensure repeatability, each test was performed 5 times and the photographic images of the water droplets after the optimized two-step protocol (HF acid etching for 25 min followed by SAM immobilization) are shown in Fig. 5b. An average contact angle larger than 160° was observed, thus confirming the feasibility of the proposed protocol to fabricate SH surfaces on SS.

Furthermore, we have also tested the durability and thermal stability of the SH surfaces on SS after several months of manufacture and storing in ambient environmental conditions and by heating it up to relatively high temperatures, respectively, as shown in Fig. 6. Five separate SS sheets were used for each test to ensure reliability. It was observed that there was no significant change in the water contact angle after 10 months of storage and exposure to temperatures ranging from 25°C up to 300 °C, thus highlighting the durability and thermal stability of the SH surfaces fabricated using the proposed two-step protocol.

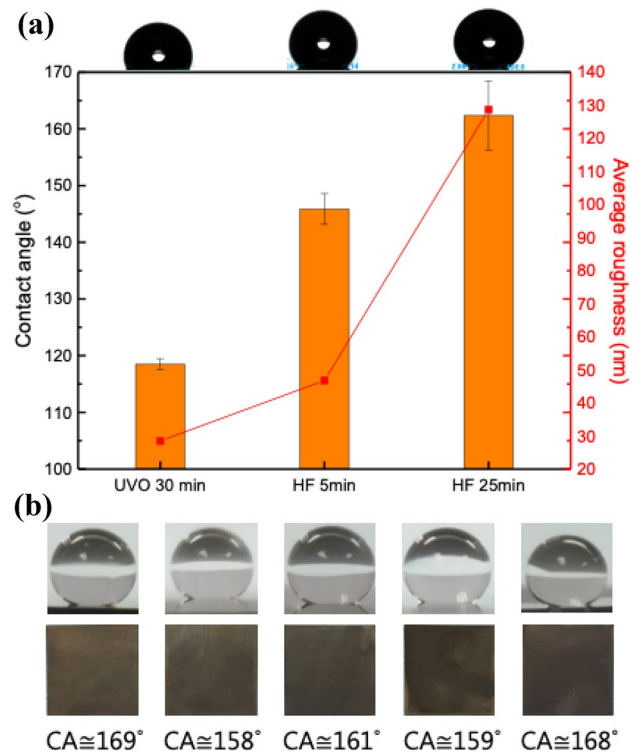


Fig. 5 **a** Final water contact angle obtained after the two-step protocol. **b** Images of the water droplet on five separate SS sheets that have been pretreated with HF acid etching for 25 min followed by SAM immobilization

3.4 IPX7 waterproof testing of SS sheets with microholes

We have also tested the feasibility of our two-step protocol to achieve IPX7 waterproofing of 304 SS sheets with microholes. Our goal was to calculate the maximum hole diameter that would prevent water from entering the microholes at hydrostatic pressures of 1 m while still allowing for air/gas permeation. Water would penetrate through the microholes if

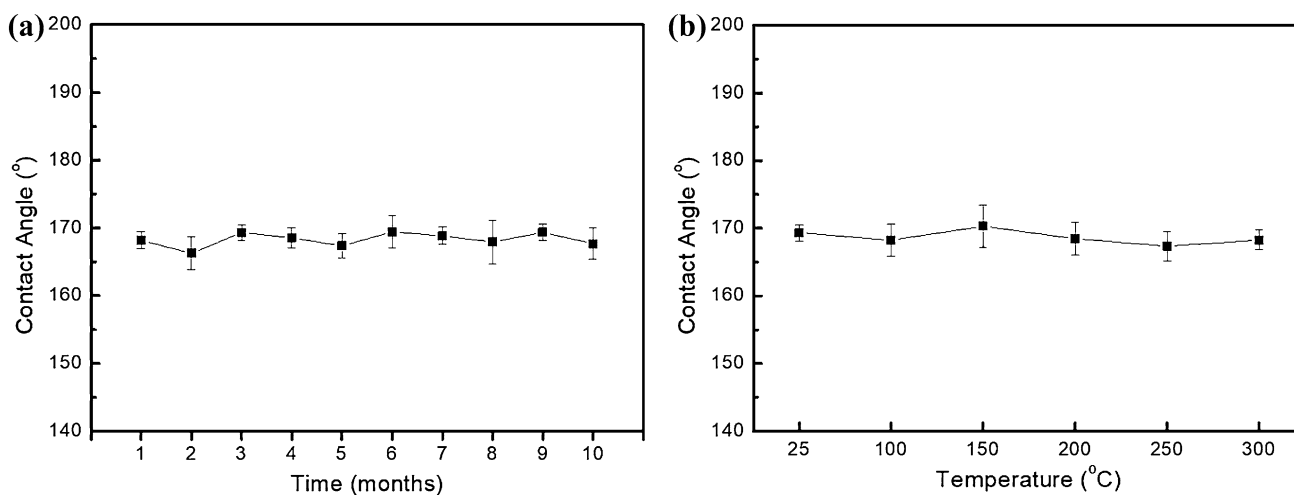


Fig. 6 The observed water contact angle after **a** 10 months of storage in air and **b** exposure to temperatures ranging from 25 °C up to 300 °C

the force exerted on the feed side is larger than the interfacial force caused by the SH coating on the SS surface. The ability of the SS sheets with microholes to resist water penetration can be described by the liquid entry pressure (LEP). LEP is the pressure that the feed water must overcome for it to penetrate through the holes and can be classically expressed by the modified Young–Laplace equation $LEP = -2\beta\gamma\cos\theta/D$ (García-Payo et al. 2000), where B is the geometric factor for the microhole shape and is 1 for perfect cylindrical holes, σ represents the surface tension of water (72.8 mN/m), θ is the water contact angle on the superhydrophobic SS surface (150° ~ 170°) and D_{max} is the maximum microhole diameter. Since we want to test for IPX7, the LEP value was chosen to be the hydrostatic pressure of water at 1 m (9.81 kPa). The resulting the d_{max} value obtained for water contact angles of 150°, 160° and 170° was calculated to be 12.91, 13.95 and 14.54 μm , respectively.

To confirm our theoretical prediction, microholes with a hole diameter of 10 μm , 25 μm and 30 μm were laser drilled

in 304 SS sheets which were then modified with our two-step protocol to enable superhydrophobicity. The resulting water contact angles for SS sheets with microholes were measured and an average water contact angle of 159°, 158.6° and 161° was observed for microholes with a diameter of 10 μm , 25 μm and 30 μm , respectively. The side and top view image of the water droplet on the SS sheets with microholes were obtained using an optical microscope as shown in Fig. 7. No significant change in contact angle was observed due to the presence of the microholes which further highlights the efficacy of our protocol. Furthermore, the results obtained after the IPX7 waterproof testing are shown in Table 1. The SS sheets with a microhole diameter of 10 μm successfully prevented water penetration during the IPX7 test with a success rate of 20% before modification with our protocol which increased to 100% after modification to obtain SH surfaces. However, 25 μm and 30 μm hole diameters could not successfully complete IPX7 testing with a failure rate of 100% before and after surface modification.

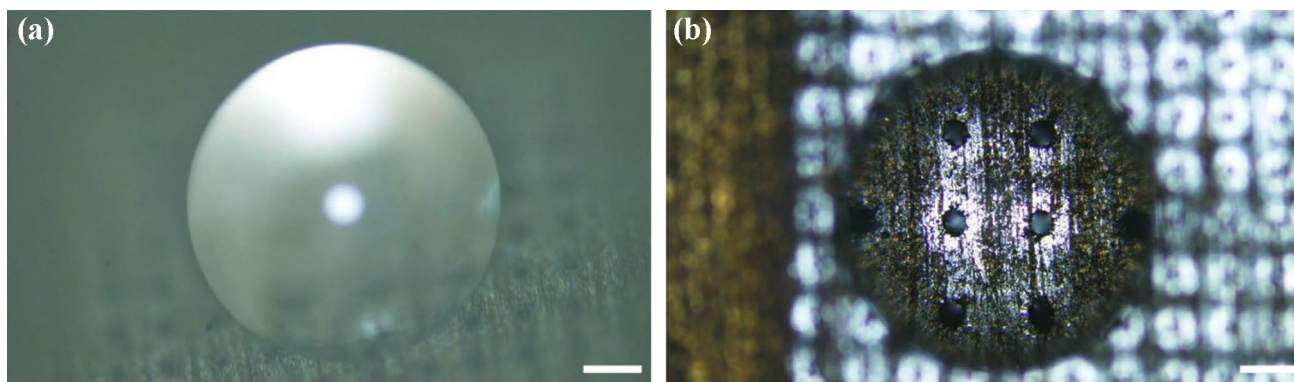


Fig. 7 The **a** side and **b** top view OM images of the water droplet on the SS sheets with microholes. The scale bar corresponds to 100 μm

Table 1 Results obtained after IPX7 waterproof testing for 304 SS sheets with microholes

Before coating		
Sample	Success/Failure	Success rate
10 μm	1/4	20%
25 μm	0/5	0%
30 μm	0/5	0%
After coating		
Sample	Success/Failure	Success rate
10 μm	5/0	100%
25 μm	0/5	0%
30 μm	0/5	0%

4 Conclusion

By utilizing a two-step protocol consisting of HF acid etching and fluorosilane SAM modification, we can successfully fabricate SH surfaces on 304 SS with achievable water contact angles up to 170° . The etching pretreatment proceeded via intergranular corrosion and the surface area increased with longer etching time due to the formation of iron and chromium fluorides. The obtained SH surfaces demonstrated durability and thermal stability with no loss in performance after several months and on exposure to temperatures as high as 300°C . Furthermore, we have successfully demonstrated the feasibility of our protocol to achieve IPX7 waterproofing for SS surfaces containing microholes with a maximum diameter of about $10\ \mu\text{m}$. The protocol proposed in this study is simple, inexpensive and scalable and can enable effective and stable fabrication of SH surfaces on SS.

Supplementary Information The online version contains supplementary material available at <https://doi.org/10.1007/s10404-021-02499-8>.

References

- Abdallah M, Benoliel C, Drider D, Dhulster P, Chihib NE (2014) Biofilm formation and persistence on abiotic surfaces in the context of food and medical environments. *Arch Microbiol* 196(7):453–472
- Ahuja A, Taylor JA, Lifton V, Sidorenko AA, Salamon TR, Lobaton EJ, Krupenkin TN (2008) Nanonails: a simple geometrical approach to electrically tunable superhydrophobic surfaces. *Langmuir* 24(1):9–14
- Barthwal S, Kim YS, Lim SH (2013) Mechanically robust superhydrophobic aluminum surface with nanopore-embedded microtexture. *Langmuir* 29(38):11966–11974
- Bhushan B, Jung YC, Niemietz A, Koch K (2009) Lotus-like biomimetic hierarchical structures developed by the self-assembly of tubular plant waxes. *Langmuir* 25(3):1659–1666
- Bixler GD, Bhushan B (2012) Bioinspired rice leaf and butterfly wing surface structures combining shark skin and lotus effects. *Soft Matter* 8(44):11271–11284
- Bormashenko E, Stein T, Whyman G, Bormashenko Y, Pogreb R (2006) Wetting properties of the multiscaled nanostructured polymer and metallic superhydrophobic surfaces. *Langmuir* 22(24):9982–9985
- Caldarelli A, Raimondo M, Veronesi F, Boveri G, Guarini G (2015) Sol–gel route for the building up of superhydrophobic nanostructured hybrid-coatings on copper surfaces. *Surf Coat Technol* 276:408–415
- Choi HJ, Shin JH, Choo S, Ryu SW, Kim YD, Lee H (2015) Fabrication of superhydrophobic and oleophobic Al surfaces by chemical etching and surface fluorination. *Thin Solid Films* 585:76–80
- Cobb HM (2010) The history of stainless steel. ASM International
- Duarte MJ, Klemm J, Klemm SO, Mayrhofer KJJ, Stratmann M, Borodin S, Renner FU (2013) Element-resolved corrosion analysis of stainless-type glass-forming steels. *Science* 341(6144):372–376
- Dunn A, Wasley TJ, Li J, Kay RW, Stringer J, Smith PJ, Shephard JD (2016) Laser textured superhydrophobic surfaces and their applications for homogeneous spot deposition. *Appl Surf Sci* 365:153–159
- Feng L, Zhang Y, Xi J, Zhu Y, Wang N, Xia F, Jiang L (2008) Petal effect: a superhydrophobic state with high adhesive force. *Langmuir* 24(8):4114–4119
- Ferroni A, Nguyen L, Pron B, Quesne G, Brusset MC, Berche P (1998) Outbreak of nosocomial urinary tract infections due to *Pseudomonas aeruginosa* in a paediatric surgical unit associated with tap-water contamination. *J Hosp Infect* 39(4):301–307
- Gao X, Jiang L (2004) Water-repellent legs of water striders. *Nature* 432(7013):36–36
- García-Payo MDC, Izquierdo-Gil MA, Fernández-Pineda C (2000) Wetting study of hydrophobic membranes via liquid entry pressure measurements with aqueous alcohol solutions. *J Colloid Interface Sci* 230(2):420–431
- Guo Z, Liu W, Su BL (2011) Superhydrophobic surfaces: from natural to biomimetic to functional. *J Colloid Interface Sci* 353(2):335–355
- Hsieh CT, Chen WY, Wu FL (2008) Fabrication and superhydrophobicity of fluorinated carbon fabrics with micro/nanoscaled two-tier roughness. *Carbon* 46(9):1218–1224
- Kavalenka MN, Vüllers F, Kumberg J, Zeiger C, Trouillet V, Stein S, Hölscher H (2017) Adaptable bioinspired special wetting surface for multifunctional oil/water separation. *Sci Rep* 7(1):1–10
- Khatak H, Raj B (eds) (2002) Corrosion of austenitic stainless steels: mechanism, mitigation and monitoring. Woodhead publishing
- Kim JH, Mirzaei A, Kim HW, Kim SS (2018) Facile fabrication of superhydrophobic surfaces from austenitic stainless steel (AISI 304) by chemical etching. *Appl Surf Sci* 439:598–604
- Kwon MH, Shin HS, Chu CN (2014) Fabrication of a superhydrophobic surface on metal using laser ablation and electrodeposition. *Appl Surf Sci* 288:222–228

- Li L, Breedveld V, Hess DW (2012) Creation of superhydrophobic stainless steel surfaces by acid treatments and hydrophobic film deposition. *ACS Appl Mater Interfaces* 4(9):4549–4556
- Li J, Jing Z, Yang Y, Wang Q, Lei Z (2014) From Cassie state to Gecko state: a facile hydrothermal process for the fabrication of superhydrophobic surfaces with controlled sliding angles on zinc substrates. *Surf Coat Technol* 258:973–978
- Liu K, Jiang L (2011) Metallic surfaces with special wettability. *Nanoscale* 3(3):825–838
- Liu K, Du J, Wu J, Jiang L (2012) Superhydrophobic gecko feet with high adhesive forces towards water and their bio-inspired materials. *Nanoscale* 4(3):768–772
- Long J, Pan L, Fan P, Gong D, Jiang D, Zhang H, Zhong M (2016) Cassie-state stability of metallic superhydrophobic surfaces with various micro/nanostructures produced by a femtosecond laser. *Langmuir* 32(4):1065–1072
- Ma M, Mao Y, Gupta M, Gleason KK, Rutledge GC (2005) Superhydrophobic fabrics produced by electrospinning and chemical vapor deposition. *Macromolecules* 38(23):9742–9748
- Martínez-Calderon M, Rodríguez A, Dias-Ponte A, Morant-Miñana MC, Gómez-Aranzadi M, Olaizola SM (2016) Femtosecond laser fabrication of highly hydrophobic stainless steel surface with hierarchical structures fabricated by combining ordered microstructures and LIPSS. *Appl Surf Sci* 374:81–89
- Nakajima A, Hashimoto K, Watanabe T, Takai K, Yamauchi G, Fujishima A (2000) Transparent superhydrophobic thin films with self-cleaning properties. *Langmuir* 16(17):7044–7047
- Nine MJ, Cole MA, Johnson L, Tran DN, Losic D (2015) Robust superhydrophobic graphene-based composite coatings with self-cleaning and corrosion barrier properties. *ACS Appl Mater Interfaces* 7(51):28482–28493
- Pan S, Kota AK, Mabry JM, Tuteja A (2013) Superomniphobic surfaces for effective chemical shielding. *J Am Chem Soc* 135(2):578–581
- Peng CW, Chang KC, Weng CJ, Lai MC, Hsu CH, Hsu SC, Yeh JM (2013) Nano-casting technique to prepare polyaniline surface with biomimetic superhydrophobic structures for anticorrosion application. *Electrochim Acta* 95:192–199
- Pozzato A, Dal Zilio S, Fois G, Vendramin D, Mistura G, Belotti M, Natali M (2006) Superhydrophobic surfaces fabricated by nanoimprint lithography. *Microelectron Eng* 83(4–9):884–888
- Qian B, Shen Z (2005) Fabrication of superhydrophobic surfaces by dislocation-selective chemical etching on aluminum, copper, and zinc substrates. *Langmuir* 21(20):9007–9009
- Shen L, Wang B, Wang J, Fu J, Picart C, Ji J (2012) Asymmetric free-standing film with multifunctional anti-bacterial and self-cleaning properties. *ACS Appl Mater Interfaces* 4(9):4476–4483
- Sun Z, Liao T, Liu K, Jiang L, Kim JH, Dou SX (2014) Fly-eye inspired superhydrophobic anti-fogging inorganic nanostructures. *Small* 10(15):3001–3006
- Wang Y, Shi Y, Pan L, Yang M, Peng L, Zong S, Yu G (2014) Multifunctional superhydrophobic surfaces templated from innately microstructured hydrogel matrix. *Nano Lett* 14(8):4803–4809
- Wang N, Xiong D, Deng Y, Shi Y, Wang K (2015) Mechanically robust superhydrophobic steel surface with anti-icing, UV-durability, and corrosion resistance properties. *ACS Appl Mater Interfaces* 7(11):6260–6272
- Wang M, Gu X, Ma P, Zhang W, Yu D, Chang P, Li D (2017a) Microstructured superhydrophobic anti-reflection films for performance improvement of photovoltaic devices. *Mater Res Bull* 91:208–213
- Wang B, Hua Y, Ye Y, Chen R, Li Z (2017b) Transparent superhydrophobic solar glass prepared by fabricating groove-shaped arrays on the surface. *Appl Surf Sci* 426:957–964
- Watson GS, Green DW, Schwarzkopf L, Li X, Cribb BW, Myhra S, Watson JA (2015) A gecko skin micro/nano structure—A low adhesion, superhydrophobic, anti-wetting, self-cleaning, biocompatible, antibacterial surface. *Acta Biomater* 21:109–122
- Wu LK, Hu JM, Zhang JQ (2013) One step sol–gel electrochemistry for the fabrication of superhydrophobic surfaces. *Journal of Materials Chemistry A* 1(46):14471–14475
- Yang Z, Wang L, Sun W, Li S, Zhu T, Liu W, Liu G (2017a) Superhydrophobic epoxy coating modified by fluorographene used for anti-corrosion and self-cleaning. *Appl Surf Sci* 401:146–155
- Yang W, Li J, Zhou P, Zhu L, Tang H (2017b) Superhydrophobic copper coating: switchable wettability, on-demand oil-water separation, and antifouling. *Chem Eng J* 327:849–854
- Yang Z, Tian YL, Yang CJ, Wang FJ, Liu XP (2017c) Modification of wetting property of Inconel 718 surface by nanosecond laser texturing. *Appl Surf Sci* 414:313–324
- Ye H, Zhu L, Li W, Liu H, Chen H (2017) Constructing fluorine-free and cost-effective superhydrophobic surface with normal-alcohol-modified hydrophobic SiO₂ nanoparticles. *ACS Appl Mater Interfaces* 9(1):858–867
- Zhang J, Sheng X, Jiang L (2009) The dewetting properties of lotus leaves. *Langmuir* 25(3):1371–1376
- Zhang J, Wang A, Seeger S (2014) Nepenthes pitcher inspired anti-wetting silicone nanofilaments coatings: preparation, unique anti-wetting and self-cleaning behaviors. *Adv Func Mater* 24(8):1074–1080
- Zhang H, Yin L, Liu X, Weng R, Wang Y, Wu Z (2016) Wetting behavior and drag reduction of superhydrophobic layered double hydroxides films on aluminum. *Appl Surf Sci* 380:178–184
- Zhang XF, Zhao JP, Hu JM (2017) Abrasion-resistant, hot water-repellent and self-cleaning superhydrophobic surfaces fabricated by electrophoresis of nanoparticles in electrodeposited sol-gel films. *Adv Mater Interfaces* 4(13):1700177
- Zhao J, Guo J, Shrotriya P, Wang Y, Han Y, Dong Y, Yang S (2019) A rapid one-step nanosecond laser process for fabrication of superhydrophilic aluminum surface. *Opt Laser Technol* 117:134–141
- Zheng B, Jiang G, Wang W, Mei X (2016) Fabrication of superhydrophilic or superhydrophobic self-cleaning metal surfaces using picosecond laser pulses and chemical fluorination. *Radiat Eff Defects Solids* 171(5–6):461–473
- Zhu Z, Xu G, An Y, He C (2014) Construction of octadecyltrichlorosilane self-assembled monolayer on stainless steel 316L surface. *Colloids Surf A* 457:408–413

Publisher's Note Springer Nature remains neutral with regard to jurisdictional claims in published maps and institutional affiliations.